MRI Acquisition and Analysis Protocol for In Vivo Intraorbital Optic Nerve Segmentation at 3T

Marios C. Yiannakas,[1,2] Ahmed T. Toosy,[1,3] Rhian E. Raftopoulos,[1,2] Raj Kapoor,[1,2] David H. Miller,[1,2] and Claudia A. M. Wheeler-Kingshott[1,2]

[1]Nuclear Magnetic Resonance Research Unit, University College London Institute of Neurology, London, United Kingdom
[2]Department of Neuroinflammation, University College London Institute of Neurology, London, United Kingdom
[3]Department of Brain Repair and Rehabilitation, University College London Institute of Neurology, London, United Kingdom

Correspondence: Marios C. Yiannakas, Nuclear Magnetic Resonance Research Unit, Department of Neuroinflammation, University College London Institute of Neurology, Queen Square House, Queen Square, London, WC1N 3BG UK; m.yiannakas@ucl.ac.uk.

Submitted: May 4, 2013
Accepted: May 14, 2013

Citation: Yiannakas MC, Toosy AT, Raftopoulos RE, Kapoor R, Miller DH, Wheeler-Kingshott CAM. MRI acquisition and analysis protocol for in vivo intraorbital optic nerve segmentation at 3T. *Invest Ophthalmol Vis Sci.* 2013;54:4235–4240. DOI:10.1167/iovs.13-12357

Purpose. To present a new acquisition and analysis protocol for reliable and reproducible segmentation of the entire intraorbital optic nerve (ION) mean cross-sectional area by means of magnetic resonance imaging (MRI) at 3 tesla (T).

Methods. Eight healthy volunteers (mean age 31, five were male) gave written informed consent and both of their IONs were imaged individually using a coronal-oblique T2-weighted fast multidynamic image acquisition scheme; the proposed acquisition scheme has its rationale in combining separately acquired volumes and registering them to account for motion-related artifacts commonly associated with longer acquisitions. Mean cross-sectional area of each ION was measured using a semiautomated image analysis protocol that was based on an active surface model previously described and used for spinal cord imaging. Reproducibility was assessed for repeated scans (scan-rescan) and repeated image analysis performance (intraobserver).

Results. Mean and SD values of the left ION cross-sectional area for the eight healthy volunteers were 5.0 ($\pm$0.7) mm^2 and for the right ION were 5.3 ($\pm$0.8) mm^2. Mean scan-rescan coefficient of variation (COV) for the left ION was 4.3% and for the right was 4.4%. Mean intraobserver COV for the left ION was 2.1% and for the right was 1.8%.

Conclusions. This study presents a new MRI acquisition and analysis protocol for reliable and reproducible in vivo measurement of the entire ION mean cross-sectional area as demonstrated in a pilot study of healthy subjects. The protocol presented here can be used in future studies of the ION in disease state.

Keywords: MRI, optic nerve, segmentation

In vivo magnetic resonance imaging (MRI) protocols that allow reliable segmentation and measurement of the mean cross-sectional area of the intraorbital optic nerve (ION) are of potential importance when studying neurological conditions, such as glaucoma[1–4] and multiple sclerosis (MS).[5–10] This is because these pathological conditions are known to involve axonal loss and progressive atrophy, with a consequent reduction in the mean cross-sectional area of the ION. Reliable measurement of ION cross-sectional area could be helpful in the early assessment of disease severity, and also could be useful as an outcome measure when assessing neuroprotective strategies.

Mean cross-sectional area has been measured over a portion of the ION by means of semiautomated image analysis of high-resolution MR images acquired with a variety of pulse sequences and image contrast, although with varying results.[5,11–16] Although the image analysis methods currently used for segmenting the ION predominantly suffer from operator-dependent errors, image acquisition strategies can be considered the more problematic aspect influencing reproducibility. For example, higher spatial resolution requires a longer acquisition time with a consequently greater risk of motion artifacts affecting especially the anterior portion of the ION[5]; faster acquisition strategies that identify surrounding cerebrospinal fluid may depict the anterior portion of the ION more clearly but can suffer from lack of conspicuity in the posterior ION region.[14] Single-slice ultrafast acquisition methods at different orthogonal positions along the length of the ION have also been used successfully, accurately addressing motion-related effects.[12,13] However, single-slice acquisitions may not be suitable in situations in which the assessment of a representative length of the ION is desired. Given the variation in length of the ION between subjects,[17] coupled with the possibility of disease manifestations (e.g., atrophy due to axonal loss) occurring variably along the length of ION, it would be preferable to acquire contiguous slices throughout the entire ION in a single imaging session.

In this work, we propose both a new image acquisition and segmentation method to cover the entire length of the ION that takes into account the technical challenges associated with imaging the ION and is based on (1) a fast multidynamic image acquisition scheme that combines separately acquired volumes and registers them to each other to account for motion-related artifacts, and (2) a semiautomated image analysis method that requires limited operator input, and that is based on an active surface model (ASM) that has been shown to be robust in measuring the spinal cord cross-sectional area,[18] a small, discrete, and cylindrical neural structure similar to the ION.

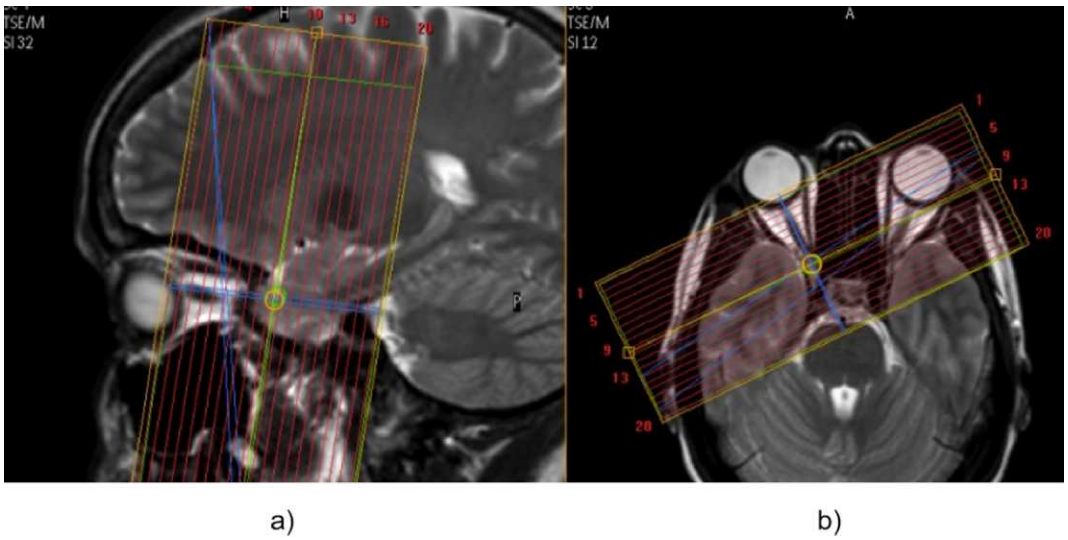

FIGURE 1. Coronal-oblique orthogonal sections through the ION facilitated by high-resolution reference images acquired in (**a**) the sagittal plane and (**b**) the axial plane; imaging of the right ION is shown in this example.

METHODS

Study Participants

Eight healthy volunteers were recruited (mean age 31 years, range, 29–33, five were male). Written informed consent was obtained from all participants. This work was approved by our local research ethics committee.

MR Imaging

A 3-tesla (T) Philips Achieva MRI system (Philips Healthcare, Best, The Netherlands) was used for this study with the manufacturer's product 32-channel head coil. For each healthy subject, the left and right IONs were imaged individually in the coronal-oblique plane to ensure the slices were orthogonal to the ION longitudinal axis in all cases. For consistent prescription of the main acquisition volume, the second slice of the volume was always positioned adjacent to the globe and this was facilitated by high-resolution reference images acquired in the sagittal and axial planes through the level of both optic nerves (see Fig. 1). The following MR sequence parameters were used for the main acquisition: a fat-suppressed heavily T2-weighted multislice "single-shot" two-dimensional (2D)-turbo spin echo with repetition time = 16 seconds; echo time = 74 ms; flip angle $\alpha = 90^{\circ}$; field of view = 160×160 mm^2; voxel size = $0.5 \times 0.5 \times 3$ mm^3; number of excitations (NEX) = 1; 20 contiguous slices (no gap); scanning time = 32 seconds per dynamic scan; number of repeated dynamic scans = 15 (total scan time 8 minutes per ION); the individual volumes acquired were then registered and added to produce the final image that was used for image segmentation and cross-sectional area measurements of the ION (see next section, "Image Analysis Protocol," for further details).

To minimize the effect of physical motion of the optic nerve during acquisition, the volunteers were verbally instructed by the MR operator to focus their vision on a colored marker positioned in front of them (i.e., straight gaze) for each one of the 32-second dynamic scans, with a short break between each dynamic scan.

Image Analysis Protocol

Image Registrations. The 15 separately acquired volumes were registered slice-by-slice using the intensity-based 2D image registration options provided by the "imregister" command in MATLAB 2012a (Mathworks, Natick, MA). Prior to the registrations, all the images were cropped to a matrix size of 31×31 pixels (see Fig. 2); this was deemed necessary due to the uncoupled motion of the ON compared with surrounding structures. A further consequence of the cropping was a considerable reduction in processing time. Using the first volume as reference, corresponding slices from each volume were then registered slice-by-slice using a 2D rigid transformation with bilinear interpolation (i.e., the transformation consisted of translation and rotation) and averaged to produce a single volume for each ION. As an example of the degree of misalignment encountered between slices prior to registration, Figure 3a demonstrates the same slice taken from each volume (in this example, slice 2; i.e., 3 mm behind the globe), binarized using Otsu's method,[19] interpolated to a higher resolution for better display and added to produce a single image; Figure 3b shows the final processed image.

Cross-Sectional Area Measurements. Using the Jim Software (available in the public domain at www.xinapse.com; Xinapse Systems, Aldwincle, UK), the ASM segmentation option was used to segment 8 to 10 slices starting immediately behind the globe up to the orbital apex; the apex level was determined by visual inspection using high-resolution sagittal images as a reference and the number of slices depended on the length of the ION between the globe and the orbital apex in each subject. Figure 4 shows an example of how the boundary of the ION was identified using the ASM segmentation option. Initially, seed points were positioned within the ION on consecutive slices and the ION contours were then identified using the ASM algorithm; following segmentation, contours were visually inspected and manually edited whenever necessary.

Reproducibility Study

Scan-rescan reproducibility was assessed by repeating the MR imaging protocol three times on five of eight volunteers, on separate occasions (with a minimum interval of 7 days and a maximum interval of 14 days between measurements), and with one experienced rater analyzing all the data. To assess the intraobserver reproducibility, the same rater reanalyzed all the data from the five volunteers' first visit three times (with the analysis performed on separate occasions after a period of at least 2 weeks between each analysis).

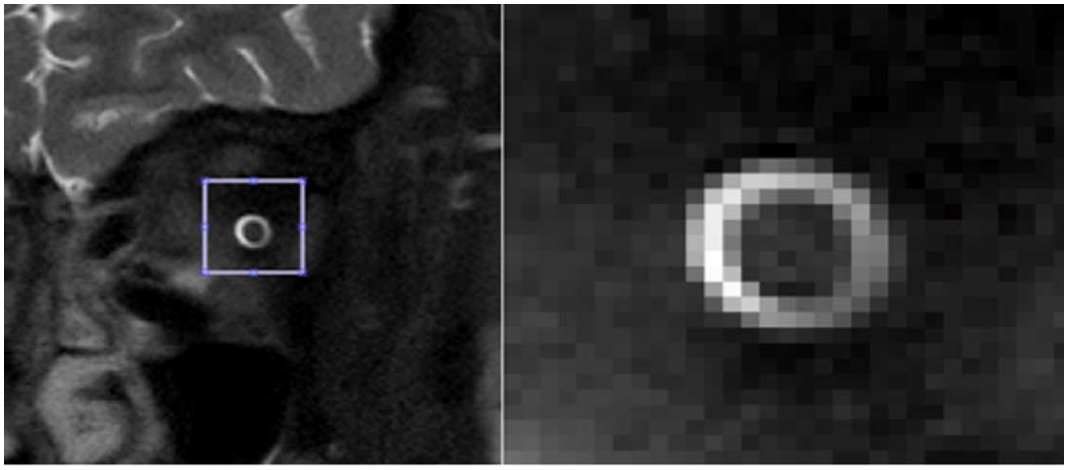

FIGURE 2. (**a**) Coronal-oblique T2-weighted image of the left ION acquired with a single dynamic scan in 32 seconds, highlighting the region that was cropped from each slice prior to the image registration step, and (**b**) the final cropped image.

Statistical Analysis

Statistical analysis was performed using the SPSS 11.0 statistical package (SPSS, Chicago, IL). For the assessment of scan-rescan and intraobserver reproducibility, the coefficient of variation (COV), expressed as a percentage, was calculated using the mean and SDs from the repeated measures using the equation $\%COV = 100 \times (SD/mean)$. For those study participants whose ION had the same length, scan-rescan COV values were reported both as an average across all slices but also on a slice-by-slice basis. Differences between left and right ION mean cross-sectional areas were investigated using paired *t*-tests and significance was accepted at P less than 0.05.

RESULTS

Image analysis was performed using all datasets without any exclusion due to motion or other artifacts. On average, image processing, which included segmentation and cross-sectional area measurements of each ION, required less than 10 minutes per side to perform for a total of 20 minutes per subject. Fewer than 20% of the contours identified using ASM required manual editing.

Mean and SD of the left ION cross-sectional area for the eight healthy volunteers was 5.0 ($\pm$0.7) mm^2 and for the right ION was 5.3 ($\pm$0.8) mm^2. Mean scan-rescan COV for the left ION was 4.3% and for the right 4.4%. Mean intraobserver COV for the left ION was 2.1% and for the right 1.8%. The Table shows more detailed results pertaining to individual sections of the left and right ION. In fact, results from the scan-rescan reproducibility assessment are shown for each individual section of the ION (i.e., slice-by-slice) for a better account on the effectiveness of the method in detecting possible localized changes. In addition, the Table shows that the mean cross-sectional area of the ION reduces as it extends from immediately behind the globe toward the orbital apex.

Statistical comparisons of mean cross-sectional area values between the left and right ION were not found to be significant.

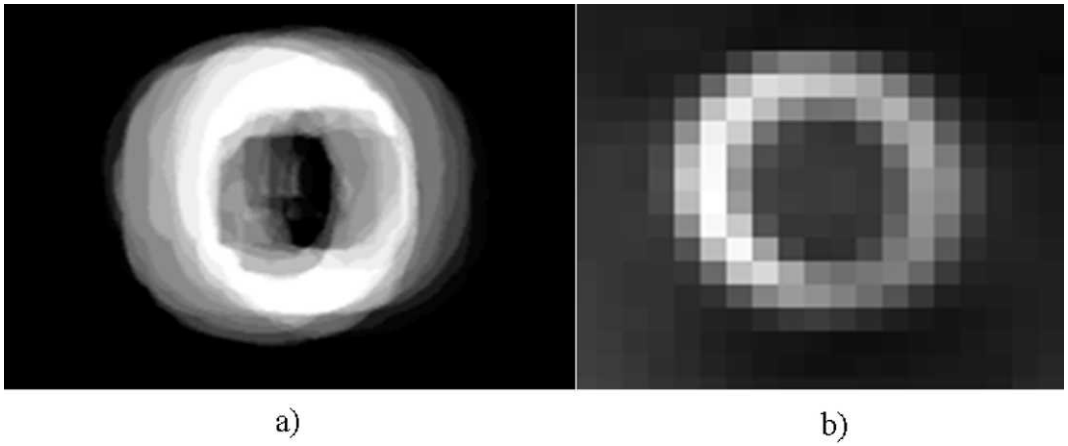

FIGURE 3. (**a**) Example of a single slice taken from repeatedly acquired volumes (i.e., each volume acquired in 32 seconds) in the anterior portion of the ION (i.e., 3 mm behind the globe) and added following interpolation and binarization; note the degree of misalignment between slices in this example, despite the cooperation of the participant by focusing his or her vision on a colored marker in straight gaze. (**b**) The final image following 2D image registration and addition of the slices.

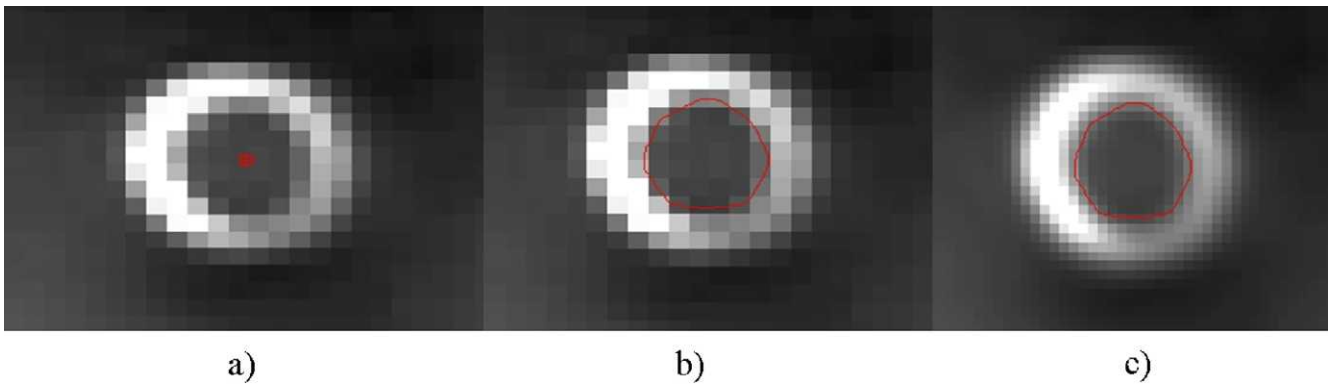

FIGURE 4. Example of the ASM segmentation method. (**a**) Single seed points were initially positioned within the ION in consecutive slices. (**b**) The boundary of the optic nerve was then identified by the algorithm; no manual intervention was required in this example following boundary identification. (**c**) Example of the final image derived from (**b**), which is shown following interpolation to higher resolution in order to improve the display.

DISCUSSION

The ability to measure the ION cross-sectional area can be invaluable when assessing certain pathological conditions.[1–10] However, current methods for measuring the ION cross-sectional area suffer from motion-related problems associated with long acquisition times and also from operator-dependent errors arising at the time of image analysis. This study has used a multidynamic acquisition scheme followed by image registration of the individual volumes into a single, more conspicuous image that was used for measuring the mean cross-sectional area of the entire ION. In addition, this study has shown that the use of a well-established image segmentation method, currently used for spinal cord cross-sectional area measurements,[18] can also be successfully applied when assessing the optic nerves.

The MR image acquisition protocol implemented in this study took into account a number of technical considerations. The choice of a coronal-oblique prescription of the imaging volume was important to ensure, as far as possible, orthogonal sections through the ION and a corresponding minimization of through-plane partial-volume effects. The use of a multidynamic acquisition scheme was important to ensure that motion-related problems, usually associated with longer acquisition times, would be considerably reduced. A key characteristic of the acquisition scheme is related to the option of adding further dynamic scans to the protocol, either in situations in which motion is identified on some of the dynamic acquisitions (i.e., in real time) or to generate an adequate signal-to-noise ratio, which in turn is affected by hardware factors, such as the scanner magnetic field strength and or head coil characteristics. In any case, the acquisition scheme presented in this study required no additional software or hardware pertaining to the MR system and, as such, this could be easily translated into the clinical setting. The method benefits from good visual fixation by the subject and this may be difficult when there is significant visual impairment.

To our knowledge, the use of ASM for segmenting the entire ION has not been reported previously; this study has shown that the segmentation worked well and should therefore be applicable in future optic nerve imaging studies that require a quantitative measure of nerve size. The method is fast, easy to use, and requires limited manual editing during the analysis. Importantly, it facilitates measurements of the mean cross-sectional area of the optic nerves, as opposed to the mean diameter, which is believed to be a more representative measure of atrophy, as has been previously described.[18] The mean intraobserver COV value of 2% (i.e., average of the left and right ION measurements) identified from the reproducibility study is favorable compared with previously reported

TABLE. Mean Cross-Sectional Area Measurements and Scan-Rescan Reproducibility Results for the Left and Right IONs in Five Healthy Volunteers*

Left ION				Right ION			
Slice No.; Distance From the Globe, mm	No. of Subjects	Mean (SD) Cross-Sectional Area, mm²	Scan-Rescan COV, %	Slice No.; Distance From the Globe, mm	No. of Subjects	Mean (SD) Cross-Sectional Area, mm²	Scan-Rescan COV, %
Slice 1; 0–3	5/5	7.8 (1.6)	3.3	Slice 1; 0–3	5/5	8 (1.5)	3.3
Slice 2; 3–6	5/5	6.2 (1.3)	9.4	Slice 2; 3–6	5/5	6.7 (0.9)	7.1
Slice 3; 6–9	5/5	5.2 (1)	8.4	Slice 3; 6–9	5/5	5.8 (0.9)	5.4
Slice 4; 9–12	5/5	4.7 (0.7)	6.2	Slice 4; 9–12	5/5	5.2 (0.9)	7
Slice 5; 12–15	5/5	4.4 (0.6)	9	Slice 5; 12–15	5/5	4.9 (0.8)	9.1
Slice 6; 15–18	5/5	4.2 (0.6)	10.6	Slice 6; 15–18	5/5	4.6 (0.6)	9.4
Slice 7; 18–21	5/5	4.1 (0.9)	8.6	Slice 7; 18–21	5/5	4.4 (0.6)	8.7
Slice 8; 21–24	5/5	3.8 (1)	4.4	Slice 8; 21–24	5/5	4.2 (0.9)	8.1
Slice 9; 24–27†	3/5	4.2 (1.6)	8.3	Slice 9; 24–27†	3/5	4.5 (1.2)	13.2

* Results shown are for each section of the ION (i.e., slice-by-slice) starting from immediately behind the globe to the apex. Reproducibility results shown are from the scan-rescan assessment.

† 3 out of 5 volunteers had slightly longer ION (i.e., from the globe to the orbital apex).

values that ranged from 2.1% to 4.8% and covered a portion of the ION only.[5,14] However, the intraobserver COV value for ION area is higher than that reported in a study measuring the healthy spinal cord cross-sectional area using the same analysis method (i.e., 0.59%).[18] This is likely to reflect the smaller size of the optic nerve and a greater potential for motion artifacts. Future work on a larger sample population will confirm the performance of the segmentation method presented here for measuring the cross-sectional area of the entire ION; further improvements are likely to depend primarily on increasing the signal-to-noise ratio and the resolution of the acquisition.

Normative mean cross-sectional area measurements of the ION obtained with the proposed acquisition and analysis protocol are in agreement with other MRI studies and reports of histomorphometry,[11–16,20] with the ION naturally reducing in diameter as it extends from the globe toward the orbital apex. However, a direct comparison of the absolute cross-sectional area values obtained in this study with the ones obtained from other studies is not straightforward. Ex vivo studies may be influenced by postmortem shrinkage, which needs to be accounted for when comparisons are made. On the other hand, in vivo MRI methodological factors, such as the type of image contrast (e.g., T1-weighted or T2-weighted), the segment of the optic nerve studied, the image resolution, and the type of image analysis, can all hinder the interpretation of normative data across different studies.

There is little doubt that for any given acquisition and analysis protocol to have successful clinical utility, certain important conditions must be met. For example, both acquisition and analysis protocols ought to be relatively time efficient and should be easily implemented without additional software or hardware requirements, but, most importantly, should provide reproducible results from repeated measurements. In this study, the mean scan-rescan COV value was calculated as 4.4%, which is lower than previously reported values of 4.9% to 6.5% using multislice acquisitions.[5,6,14] Given that ION atrophy ranging from 10% to 30% is described following optic neuritis,[6,10] a scan-rescan COV of 4% to 5% should be acceptable for clinical application. However, there is scope for improving this result and it would be desirable to do so. Image resolution is currently the main limiting factor, hence future work should be directed at improving signal-to-noise ratio, possibly by evaluating different coil designs as well as further refining the acquisition scheme (e.g., investigating fast three-dimensional acquisition modes).

The ability to detect small changes in cross-sectional area of the ION may have important implications for monitoring disease changes. However, cross-sectional area measurements in disease state may prove less straightforward than the study of healthy subjects. For example in MS, following an episode of optic neuritis, there is initial swelling of the optic nerve (hence increase ION) due to inflammation, with evolution to atrophy at a later stage.[5,6] It is therefore suggested that studies are conducted specifically to assess the potential value of the method presented here for measuring atrophy in longitudinal studies of optic neuritis and compared with other approaches,[5–10] including the measurement of retinal nerve fiber layer thickness using optic coherence tomography (OCT).[21,22] Although OCT is a robust and reproducible measure of axonal loss following optic neuritis, it does not study the symptomatic lesion per se, and unlike the retina, the optic nerve contains myelin as well as axons, and, importantly, both of these tissue elements contribute to the ION area measure and are crucial in allowing normal salutatory nerve conduction. Thus, continued efforts are warranted to improve the quality of optic nerve imaging, and to accurately and efficiently measure ION area. The most important quality of the present acquisition and analysis protocol, besides the improved reproducibility, is the fact that the entire ION can be assessed in a single imaging session, unlike existing imaging protocols that do not routinely offer this option.

In summary, this study defines a new MRI acquisition and analysis protocol that allows for the first time reliable and reproducible measurement of the mean cross-sectional area of the entire ION in vivo at 3 T. The protocol is feasible to use in the clinical setting to study pathological conditions that affect the ION.

Acknowledgments

Supported by the Multiple Sclerosis Society of Great Britain and Northern Ireland and the Department of Health's Comprehensive Biomedical Research Centre at University College Hospitals Trust; both also support the Nuclear Magnetic Resonance Research Unit.

Disclosure: **M.C. Yiannakas**, None; **A.T. Toosy**, None; **R.E. Raftopoulos**, None; **R. Kapoor**, None; **D.H. Miller**, None; **C.A.M. Wheeler-Kingshott**, None

References

1. Lagrèze WA, Gaggl M, Weigel M, et al. Retrobulbar optic nerve diameter measured by high-speed magnetic resonance imaging as a biomarker for axonal loss in glaucomatous optic atrophy. *Invest Ophthalmol Vis Sci*. 2009;50:4223–4228.
2. Beatty S, Good PA, McLaughlin J, O'Neill EC. Echographic measurements of the retrobulbar optic nerve in normal and glaucomatous eyes. *Br J Ophthalmol*. 1998;82:43–47.
3. Stroman GA, Stewart WC, Golnik KC, Curé JK, Olinger RE. Magnetic resonance imaging in patients with low-tension glaucoma. *Arch Ophthalmol*. 1995;113:168–172.
4. Kashiwagi K, Okubo T, Tsukahara S. Association of magnetic resonance imaging of anterior optic pathway with glaucomatous visual field damage and optic disc cupping. *J Glaucoma*. 2004;13:189–195.
5. Hickman SJ, Brex PA, Brierley CMH, et al. Detection of optic nerve atrophy following a single episode of unilateral optic neuritis by MRI using a fat-saturated short-echo fast FLAIR sequence. *Neuroradiology*. 2001;43:123–128.
6. Hickman SJ, Toosy AT, Jones SJ, et al. A serial MRI study following optic nerve mean area in acute optic neuritis. *Brain*. 2004;127:2498–2505.
7. Hickman SJ. Optic nerve imaging in multiple sclerosis. *J Neuroimaging*. 2007;17:42S–45S.
8. Hickman SJ, Miszkiel KA, Plant GT, Miller DH. The optic nerve sheath on MRI in acute optic neuritis. *Neuroradiology*. 2005; 47:51–55.
9. Inglese M, Ghezzi A, Bianchi S, et al. Irreversible disability and tissue loss in multiple sclerosis: a conventional and magnetization transfer magnetic resonance imaging study of the optic nerves. *Arch Neurol*. 2002;59:250–255.
10. Trip SA, Schlottmann PG, Jones SJ, et al. Optic nerve atrophy and retinal nerve fibre layer thinning following optic neuritis: evidence that axonal loss is substrate of MRI-detected atrophy. *Neuroimage*. 2006;31:286–293.
11. Karim S, Clark RA, Poukens V, Demer JL. Demonstration of systematic variation in human intraorbital optic nerve size by quantitative magnetic resonance imaging and histology. *Invest Ophthalmol Vis Sci*. 2004;45:1047–1051.
12. Weigel M, Lagrèze WA, Lazzaro A, Hennig J, Bley TA. Fast and quantitative high-resolution magnetic resonance imaging of the optic nerve at 3.0 tesla. *Invest Radiol*. 2006;41:83–86.
13. Lagrèze WA, Lazzaro A, Weigel M, Hansen HC, Hennig J, Bley TA. Morphometry of the retrobulbar human optic nerve: comparison between conventional sonography and ultrafast magnetic resonance sequences. *Invest Ophthalmol Vis Sci*. 2007;48:1913–1917.

14. Yiannakas MC, Wheeler-Kingshott CA, Berry AM, et al. A method for measuring the cross sectional area of the anterior portion of the optic nerve in vivo using a fast 3D MRI sequence. *J Magn Reson Imaging*. 2010;31:1486–1491.
15. Ozgen A, Aydingöz U. Normative measurements of orbital structures using MRI. *J Comput Assist Tomogr*. 2000;24:493–496.
16. Bert RJ, Patz S, Ossiani M, et al. High-resolution imaging of the human eye 2005. *Acad Radiol*. 2006;13:368–378.
17. Walsh FB. The visual sensory system. In: FB, Walsh, Hoyt WF, eds. *Clinical Neuro-ophthalmology*. 3rd ed. Baltimore, MD: Williams and Wilkins; 1969:1–129.
18. Horsfield MA, Sala S, Neema M, et al. Rapid semi-automatic segmentation of the spinal cord from magnetic resonance images: application in multiple sclerosis. *Neuroimage*. 2010; 50:446–455.
19. Otsu N. A Threshold Selection Method from Gray-Level Histograms. *IEEE Trans Syst Man Cybern*. 1979;9:62–66.
20. Jonas JB, Müller-Bergh JA, Schlötzer-Schrehardt UM, Naumann GO. Histomorphometry of the human optic nerve. *Invest Ophthalmol Vis Sci*. 1990;31:736–744.
21. Henderson AP, Altmann DR, Trip AS, et al. A serial study of retinal changes following optic neuritis with sample size estimates for acute neuroprotection trials. *Brain*. 2010;133: 2592–2602.
22. Petzold A, de Boer JF, Schippling S, et al. Optical coherence tomography in multiple sclerosis: a systematic review and meta-analysis. *Lancet Neurol*. 2010;9:921–932.

Investigative Ophthalmology & Visual Science